Journal of Veterinary Internal Medicine
Open Access

J Vet Intern Med 2016;30:1099–1111

Endothelin-1 Immunoreactivity and its Association with Intramedullary Hemorrhage and Myelomalacia in Naturally Occurring Disk Extrusion in Dogs

D. Mayer, A. Oevermann, T. Seuberlich, M. Vandevelde, A. Casanova-Nakayama, S. Selimovic-Hamza, F. Forterre, and D. Henke

Background: The pathophysiology of ascending/descending myelomalacia (ADMM) after canine intervertebral disk (IVD) extrusion remains poorly understood. Vasoactive molecules might contribute.

Hypothesis/Objectives: To investigate the immunoreactivity of endothelin-1 (ET-1) in the uninjured and injured spinal cord of dogs and its potential association with intramedullary hemorrhage and extension of myelomalacia.

Animals: Eleven normal control and 34 dogs with thoracolumbar IVD extrusion.

Methods: Spinal cord tissue of dogs retrospectively selected from our histopathologic database was examined histologically at the level of the extrusion (center) and in segments remote from the center. Endothelin-1 immunoreactivity was examined immunohistochemically and by in situ hybridization. Associations between the immunoreactivity for ET-1 and the severity of intramedullary hemorrhage or the extension of myelomalacia were examined.

Results: Endothelin-1 was expressed by astrocytes, macrophages, and neurons and only rarely by endothelial cells in all dogs. At the center, ET-1 immunoreactivity was significantly higher in astrocytes (median score 4.02) and lower in neurons (3.21) than in control dogs (3.0 and 4.54) ($P < .001$; $P = .004$) irrespective of the grade of hemorrhage or myelomalacia. In both astrocytes and neurons, there was a higher ET-1 immunoreactivity in spinal cord regions remote from the center (4.58 and 4.15) than in the center itself ($P = .013$; $P = .001$). ET-1 mRNA was present in nearly all neurons with variable intensity, but not in astrocytes.

Conclusion and Clinical Importance: Enhanced ET-1 immunoreactivity over multiple spinal cord segments after IVD extrusion might play a role in the pathogenesis of ADMM. More effective quantitative techniques are required.

Key words: Dog; Intramedullary hemorrhage; IVD extrusion; Myelomalacia.

Spinal cord injury (SCI) after intervertebral disk (IVD) extrusion is a common disease in dogs and leads to tissue damage ranging from mild changes of gray and white matter to significant structural destruction and softening of the spinal cord tissue, the so-called myelomalacia.[1,2] Myelomalacia can remain focal at the IVD extrusion site or might ascend, descend, or both into adjacent spinal cord segments or even the whole spinal cord.[3–5]

After the primary mechanical insult, secondary mechanisms including decreased vascular perfusion followed by ischemia and perivascular edema, electrolyte imbalances, glutamatergic excitotoxicity, oxidative stress, inflammation, and apoptosis lead to further damage of the spinal cord parenchyma.[6,7] Additionally, in connection with hemorrhage resulting from primary or secondary spinal cord injury, vasoactive molecules contribute to further disruption of the blood spinal cord barrier (BSCB).[8] Several underlying molecular mechanisms have been investigated in this respect experimentally such as overexpression of the Sur1-Trpm4 channel[9–11] and of endothelin-1 (ET-1).[12]

Among the three ET isoforms, ET-1 is the most abundant and physiologically relevant form, and is expressed in liver, lung, kidneys, brain and spinal cord and binds to either the ET_A or ET_B receptor.[13–16] It is a potent vasoconstrictor.[17,18] The vasoactive function of

Abbreviations:

IVD	intervertebral disk
ET-1	endothelin-1
SCI	spinal cord injury
ADMM	ascending/descending myelomalacia
BSCB	blood spinal cord barrier
ISH	*in situ* hybridization
IHC	immunohistochemistry
DEPC	diethylpyrocarbonate
PBS	phosphate-buffered saline
RT	room temperature

From the Division of Neurological Sciences, (Mayer, Oevermann, Seuberlich, Vandevelde, Forterre, Henke); the Division of Clinical Neurology, (Mayer, Vandevelde, Henke); the Department of Clinical Veterinary Medicine, (Mayer, Vandevelde, Forterre, Henke); the Department of Clinical Research and Veterinary Public Health, (Oevermann, Seuberlich, Selimovic-Hamza); the Centre for Fish and Wildlife Health, Institute of Animal Pathology, (Casanova-Nakayama); and the Division of Small Animal Surgery, Vetsuisse Faculty, University of Bern, Bern, Switzerland (Forterre).

The study was performed at the University of Bern, Vetsuisse Faculty, Switzerland. The study was supported by the Department of Clinical Veterinary Medicine of the University of Bern and by the Burgergemeinde Bern. The local ethical authorities at the Vetsuisse Faculty, University of Bern, approved the study. Parts of this study were presented at the annual ECVN meeting 2015 in Amsterdam.

Corresponding author: D. Henke, Division of Neurological Sciences, Department of Clinical Veterinary Medicine, Laenggassstrasse 128, 3001 Bern, Switzerland; e-mail: diana.henke@vetsuisse.unibe.ch.

Submitted August 15, 2015; Revised March 4, 2016; Accepted May 23, 2016.

DOI: 10.1111/jvim.14364

ET-1 is mediated by G protein-coupled endothelin receptors, ET_A and ET_{B2}, in smooth muscle cells of blood vessels,[18] and is thought to lead to vasospasm resulting in ischemic damage to neurons.[8,19,20] On the other hand, binding of ET-1 to the ET_{B1} receptor on endothelial cells leads to vasodilatation via generation of NO.[18]Additionally, the ET_B receptor has been shown to be expressed on radial glia cells, ependymal cells, vascular endothelial cells, and astrocytes in rodents.[16] ET-1 regulates several astroglial functions among others mitogenesis, intracellular Ca2+ levels, glutamate efflux, and synthesis of inflammatory mediators.[21–24]

The formation of ET-1 is stimulated by oxyhemoglobin either derived from the injured tissue itself, or from red blood cells after disruption of blood vessels a frequent complication of SCI.[12,20,25] In experimental SCI in rats, ET-1 synthesis is initially upregulated in neurons and endothelial cells[26,27] and delayed in reactive astrocytes.[24,28]

The pathophysiology of ascending/descending myelomalacia (ADMM) after IVD extrusion remains poorly understood. Even though intramedullary hemorrhage is a very common finding[5,29,30] and is associated with the severity of spinal cord damage in the center and the longitudinal extension of myelomalacia,[5] the precise mechanism how hemorrhage could induce progressive extension of myelomalacia in dogs after IVD extrusion remains unknown. Since oxyhemoglobin stimulates the expression of ET-1, a potent vasoconstrictor and regulator of astrocytic functions, we hypothesize that intramedullary hemorrhage upregulates the expression of ET-1 which could be detrimental to the spinal cord parenchyma leading to further extension of myelomalacia. Therefore, the purpose of the present study was to investigate the immunoreactivity of ET-1 in the uninjured and injured canine spinal cord and its potential association with intramedullary hemorrhage and severity of myelomalacia with special emphasis on ADMM, by semiquantitative immunohistochemistry (IHC) and in situ hybridization (ISH).

Materials and Methods

Histopathologic examination of the spinal cord was performed in 34 dogs with thoracolumbar IVD extrusion which were euthanized between January 1991 and December 2014 at the veterinary teaching hospital of the University of Bern. Inclusion criteria were well-documented records of the neurologic history, and availability of histologic sections of the entire spinal cord.

Additionally, 11 dogs without clinical signs of a spinal cord pathologies and histologic changes, which had been euthanized because of other pathologies, were included as controls.

Clinical Data

Data collected from the medical records included breed, age, sex, duration and severity of clinical signs, and treatment.

Duration of neurologic signs was defined as the time between the first observed clinical signs and euthanasia, and was categorized as follows: euthanasia within the first 24 hours after onset of signs (acute), between 25 hours and 7 days after onset (subacute), or after more than 7 days (chronic) according to previous studies.[31]

A complete neurologic examination was performed maximally 12 hours before euthanasia. Neurological condition was graded on a I–V scale as published before[31]; grade I: spinal hyperesthesia only; grade II: ambulatory paraparesis and ataxia or ataxia, and proprioceptive or proprioceptive; deficits, grade III: nonambulatory paraparesis; grade IV: paraplegia with present nociception; grade V: paraplegia with loss of nociception.

Histopathologic Examination

The processing of the material followed the same established standardized protocol in all dogs.

The spinal cord was removed within 12 hours after euthanasia in all affected as well as control dogs (ranging from 2 hours to 12 hours), and then fixed in 10% formalin. For gross inspection, the fixed spinal cord was cross-sectioned at multiple levels; namely at the site of the IVD extrusion ("center"), the immediately adjacent segments on either side of the center, additional segments of the spinal cord exhibiting macroscopic changes, and finally more remote proximal and distal segments without grossly visible lesions including the upper cervical spinal cord, cervical intumescence, and lumbar intumescence. In control dogs, the spinal cord was cross-sectioned at different levels including the upper cervical spinal cord, cervical intumescence, thoracolumbar spinal cord and lumbar intumescence. Cross-sectioned blocks of these levels were embedded in paraffin wax within 14 days, after a standard protocol, and sections of 5 μm were cut from all samples and stained with hematoxylin and eosin for histopathologic assessment. The number of transverse sections cut and stained ranged from 10 to 30 and depended on the longitudinal extension of the lesion.

Semiquantitative Assessment of Spinal Cord Damage and Hemorrhage

All slides were examined and graded independently by two experienced observers (DH, MV). If discordance occurred between the observers, slides were re-examined and consensus was agreed.

To evaluate the longitudinal extension of the lesion, the presence of myelomalacia, defined as complete loss of structural integrity of spinal cord parenchyma, was assessed on all sections of each animal, thus including the center, adjacent and more remote spinal cord segments. The longitudinal extension was categorized as grade 0 (no malacia), grade 1 (focal malacia at the center), and grade 2 (ADMM from the center across at least 3 spinal cord segments) as previously described and illustrated.[5]

Intramedullary hemorrhage was categorized as grade 0 (no hemorrhage), grade 1 (scattered ring hemorrhages), grade 2 (coalescing ring hemorrhages and diffuse spread of erythrocytes in the parenchyma), or grade 3 (mass hemorrhage) as previously described and illustrated.[5]

Immunohistochemistry

Paraffin-embedded spinal cord sections were immunostained for ET-1. Native slides were deparaffinized using xylene, rehydrated in graded ethanol, pretreated with heat-induced antigen retrieval in citrate buffer (pH = 6) at 95°C for 20 minutes using a laboratory microwave. Sections were blocked with 10% normal goat serum for 2 hours at room temperature (RT), and then incubated with antibodies against ET-1 (monoclonal mouse; 1 : 350 dilution; Abcam; the antibody had been predicted by the provider to bind to canine ET-1) for 12 hours at 4°C. Subsequently, endogenous peroxidase was blocked with 3% H_2O_2 in methanol over 15 minutes at RT. Then, slides were incubated with biotinylated goat anti-mouse IgG (1 : 1000, Milan Analytica) for 1 hour, and thereafter with peroxidase-streptavidin (1 : 1000, Milan Analytica) for

30 minutes at RT. Immunohistochemical staining was visualized by incubating the slides with 3-amino-9-ethylcarbazole for 6–8 minutes at RT, and by counterstaining with Mayer's hematoxylin. Sections from canine liver tissue treated in the same way served as positive controls. Negative controls were performed using nonspecific mouse IgG instead of the primary antibody in the same concentration on both canine liver tissue and on spinal cord sections.

Qualitative and Semiquantitative Assessment of Immunohistochemistry

Immunohistochemical staining of blinded spinal cord sections from dogs with IVD extrusion and control dogs was evaluated and graded by 2 observers (DM, DH) independently. In cases of disagreement between them, the slides were re-evaluated and consensus was agreed.

Every animal was evaluated at two spinal cord levels, including a cross-section of the cord at the level of the IVD extrusion, either in the center or in a directly adjacent segment if the former was completely necrotic. In addition, a cross-section of the cord remote from the IVD extrusion site was examined: the section with the lowest level of histopathological parenchymal damage of all available spinal cord sections was selected.

Positively stained astrocytes were identified according to their large cytoplasm, clear nucleus, and star-shaped cell processes. The number of positively stained astrocytes in the white matter of the selected cord sections was counted in three different randomized visual fields at 40× magnification, and then summated and categorized into four grades: grade 1 (≤20 positively stained astrocytes per visual field), grade 2 (21–40), grade 3 (41–60), and grade 4 (61–80). In case of severe tissue destruction in the center, the closest adjacent segment revealing preserved white matter parenchyma in at least 3 visual fields (without malacia) was used.

The percentage of positively stained large neurons in the gray matter of the ventral horns and intermedio-lateral horns was categorized in 3 grades: grade 1 (<50% of the neurons positively stained), grade 2 (50–75%), and grade 3 (>75%).

The intensity of the IHC staining of the different cell types was judged against defined standard sections and assessed as grade 0 (no staining), grade 1 (mild), grade 2 (moderate), and grade 3 (strong) (Fig 1).

Finally, the ET-1 immunoreactivity of astrocytes was demonstrated as a score after summation of number and intensity grades (ET-1 immunoreactivity score astrocytes = grade "number of positively stained astrocytes" + grade "intensity of astrocytic staining").

The same was calculated for the ET-1 immunoreactivity of neurons.

Statistical Analyses

The after associations were statistically evaluated using a Kruskal-Wallis test on Ranks test with Bonferroni correction for multiple comparisons: the association between ET-1 immunoreactivity (in both the center and remote from the center) and (1) grade of intramedullary hemorrhage, (2) degree of longitudinal extension of myelomalacia as evaluated on sequential sections, and (3) duration of clinical signs. In addition, ET-1 immunoreactivity at the level of the IVD extrusion was compared to the ET-1 immunoreactivity in spinal cord segments remote from the IVD extrusion site.

For statistical analyses, hemorrhage grades of 0 and 1; neuronal ET-1 immunoreactivity grade of 1 and 2, and of grade 5 and 6; and astrocytic ET-1 immunoreactivity grade of 2 and 3, and of grade 6 and 7 were grouped together because of the small sample numbers (Table S1). The threshold for statistical significance was set to $P < .05$. All statistical analyses were performed using a statistical software package (NCSS 2009, www.ncss.com).

Probe Production for In Situ Hybridization

For generating a RNA probe to detect mRNA of ET-1 in formalin-fixed paraffin-embedded tissues of dogs, a 400 bp DNA fragment of the ET-1 gene was synthesized (Eurofins, Germany).

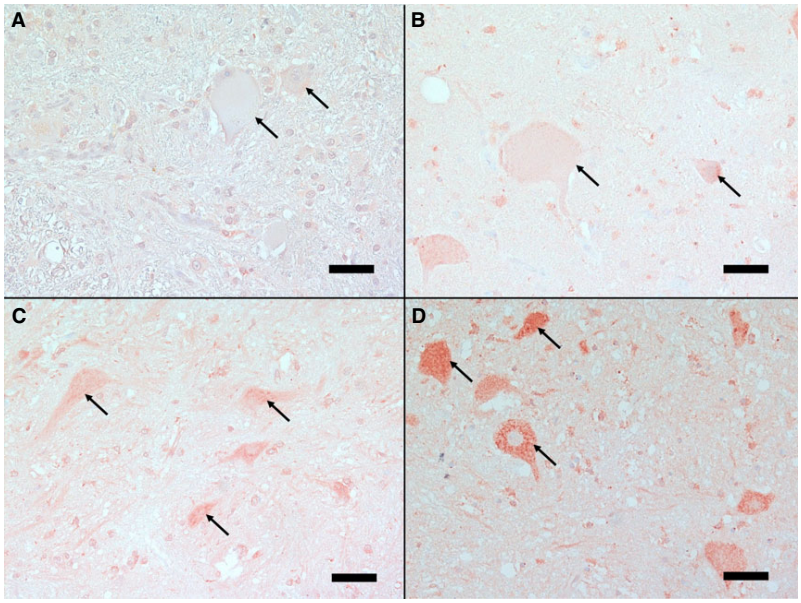

Fig 1. Spinal cord cross-sections showing different intensities of immunohistochemical staining for endothelin-1 in neurons. Standard sections of different staining intensities of neurons (arrows) are presented: **A-** Grade 0: no positive staining, **B-** Grade 1: mild positive staining, **C-** Grade 2: moderate positive staining, and **D-** Grade 3: strong positive staining, note the distinct granular cytoplasmatic staining. (IHC, bar = 50 μm)

This fragment corresponded to the sequence of nucleotides 481–880 of the canine mRNA for preproendothelin-1 available in the NCBI gene bank (access number: AB115087.1). The fragment contained additional 5′ and 3′ sequences for the restriction enzymes BamHI (GGATCC) and EcoRI (GAATTC), respectively, and was cloned into the pSPT18 plasmid (Roche). The resulting plasmid pSPT-18_ET-1 was transfected into bacteria (XL10-Gold Ultracompetent Cells, Agilent). The inserted sequence was confirmed by PCR-screening and DNA sequencing.

For in-vitro transcription of digoxigenin (DIG)-labeled RNA, pSPT-18_ET-1 was linearized with BamHI for the antisense probe or EcoRI for the sense probe, respectively.

The RNAs were transcribed from the linearized plasmids with the DIG-RNA Labeling Kit (Roche Applied Science) according to the manufacturer's recommendations. In order to remove remaining DNA, the reactions were treated with DNase I (15 minutes, 37°C) and purified by ethanol precipitation. T7 RNA polymerase served to transcribe the antisense probe and SP6 RNA polymerase the sense probe.[32,33] Agarose gel electrophoresis was used to estimate the amount of probes for in situ hybridization. The probes were stored at −20°C.

In Situ Hybridization

Liver and selected spinal cord sections were deparaffinized with xylene and rehydrated through graded ethanol. Afterward, slides were incubated in diethylpyrocarbonate (DEPC) water (5 minutes, RT), phosphate-buffered saline (PBS) (5 minutes, RT), and 0.2M HCl for denaturation (20 minutes, RT). Between all steps sections were rinsed with 2× SSC (sodium chloride/sodium citrate buffer) in DEPC water. Slides were then treated with proteinase K (1.12–1.76 μg/mL) solution (15 minutes, 37°C) and proteinase activity was blocked by 0.2% glycine in PBS (2 minutes, RT). Additionally, slides were incubated in 4% paraformaldehyde to denature proteinase K and to refixate the tissue (5 minutes, RT).

A pretreatment with acetic anhydride (0.25%) in triethanolamine was used to reduce the background staining and to inactivate RNases (15 minutes, 37°C). Sections were then incubated in prehybridization solution (4× SSC, 50% formamide, 2× Denhardt's, 10 mg/mL yeast RNA) (2 hour, 50°C). The slides were incubated overnight with probes (final concentration: 50.9–80.0 μg/mL) in hybridization buffer (4× SSC, 50% formamide, 2× Denhardt's, 10 mg/mL yeast RNA, 10% dextran sulfate) covered with GelBonds at 50°C in a humidified box. Slides were then treated with RNase (200 U/mL RNase T1 and 0.2 μg/mL RNase DNase-free, Roche) at 37°C for 30 minutes and washed with 2× SSC and 0.2× SSC (10 minutes, 55°C). First 10% blocking buffer (Roche) and afterward BSA-TritonX-100 solution (0.1 mM Tris-HCl and 0.15 M NaCl with 1% BSA and 0.3% TritonX-100) were used for blocking. Anti-DIG-antibodies conjugated with alkaline phosphatase (1 : 3000, Roche) in BSA-TritonX-100 were used to detect DIG-labeled RNA probes. After washing the sections with BSA-TritonX-100 solution and a buffer (10 mM Tris, 10 mM NaCl and 50 mM $MgCl_2$*$6H_2O$; pH = 9.5), slides were incubated with NBT/BCIP (5-bromo-4-chloro-3-indolyl phosphate and nitro blue tetrazolium) overnight in the dark covered with GelBonds. The reaction was stopped with 0.01 M TrisHCl and 1 mM EDTA (10 minutes, RT, dark).

The type of positively stained cells was determined according to their phenotype.

Results

Clinical data

Thirty-four dogs met the inclusion criteria. In all of these dogs, histologic examination and IHC for ET-1 was done. Spinal cords of 25 of these 34 dogs were additionally analyzed by ISH. These breeds were included; Affected group: 7 French bulldog, 4 mixed-breed dogs, 3 German Shepherd dogs, 2 Border collie, 2 Dachshund, 2 Lhasa Apso, and 1 each of Alaskan Malamute, Beagle, Cavalier King Charles spaniel, Chin chinois, Cocker spaniel, Coton de Tulear, German spaniel, Jack Russel Terrier, Labrador retriever, Mallinois, Pekingese, Shih Tzu, Tibet Terrier, and Yorkshire Terrier.

Ages of the diseased dogs ranged from 3 to 14 years (mean 6.4 years). Eighteen dogs were male intact, 3 male castrated, 8 female intact, and 5 female spayed.

The mean duration of clinical signs was 10 days (range 1–90 days), and the clinical signs were classified as acute in 5 dogs, subacute in 17 dogs, and chronic in 12 dogs accordingly.

Fifteen dogs were euthanized at the request of the owners because of initial poor prognosis. Fifteen dogs received decompressive surgery (hemilaminectomy) and 4 dogs were treated conservatively. These dogs were euthanized because of lack of improvement or deterioration of clinical signs.

The neurological status before euthanasia was grade II in 1, grade III in 3, grade IV in 6, and grade V in 24 dogs. Four dogs of the latter group developed clinical signs of ADMM (involvement of thoracic limbs, reduced segmental spinal reflexes of pelvic limbs) (Table 1).

Additionally, 11 control dogs of different breeds were included: 2 Golden Retrievers, 2 mixed-breed dogs, and 1 each of Bernese mountain dog, Bichon frise, Dachshund, French bulldog, Lhasa apso, Pug dog, and Samojede.

Ages ranged from 1 month to 11 years (mean 5.3 years). Seven dogs were male intact and 4 female intact.

Histopathological Findings

All dogs exhibited spinal cord lesions at the center with varying degrees of edema of the parenchyma, axonal swelling, neuronal necrosis, invasion of neutrophils, and macrophages. In cases with severe tissue destruction in the center, the spinal cord tissue was replaced by an amorphous mixture of spinal cord tissue debris, macrophages, and blood. In those dogs, this hemorrhagic necrotic material was also found inside or dorsal to the central canal, or both in spinal cord segments distant from the center of the lesion in otherwise mildly damaged spinal cord tissue as described previously.[5] Gliosis and vascular proliferation were present in chronic cases. The severity of the spinal cord lesions generally correlated well with the neurological grades at the time of euthanasia as reported before.[2]

In all but 9 dogs, areas of myelomalacia (complete lysis of spinal cord tissue) of varying size were seen on cross-sections (Fig 2A1). On longitudinal assessment, myelomalacia extended from the center into the neighboring segments in many animals. Accordingly, the grade of myelomalacia was classified as focal

Table 1. Distribution of intramedullary hemorrhage grades and grades of myelomalacia in respect to the neurological grades in 34 dogs with intervertebral disk extrusion.

		Myelomalacia Number of Dogs			Hemorrhage Number of Dogs			
Clinical grade	Number of Dogs	No	Focal	ADMM	No	Scattered ring	Coalescing ring	Mass
II	1	0	1	0	1	0	0	0
III	3	2	1	0	0	2	1	0
IV	6	3	2	1	0	4	0	2
V	24	4	7	13	3	4	12	5
Total	34	9	11	14	4	10	13	7

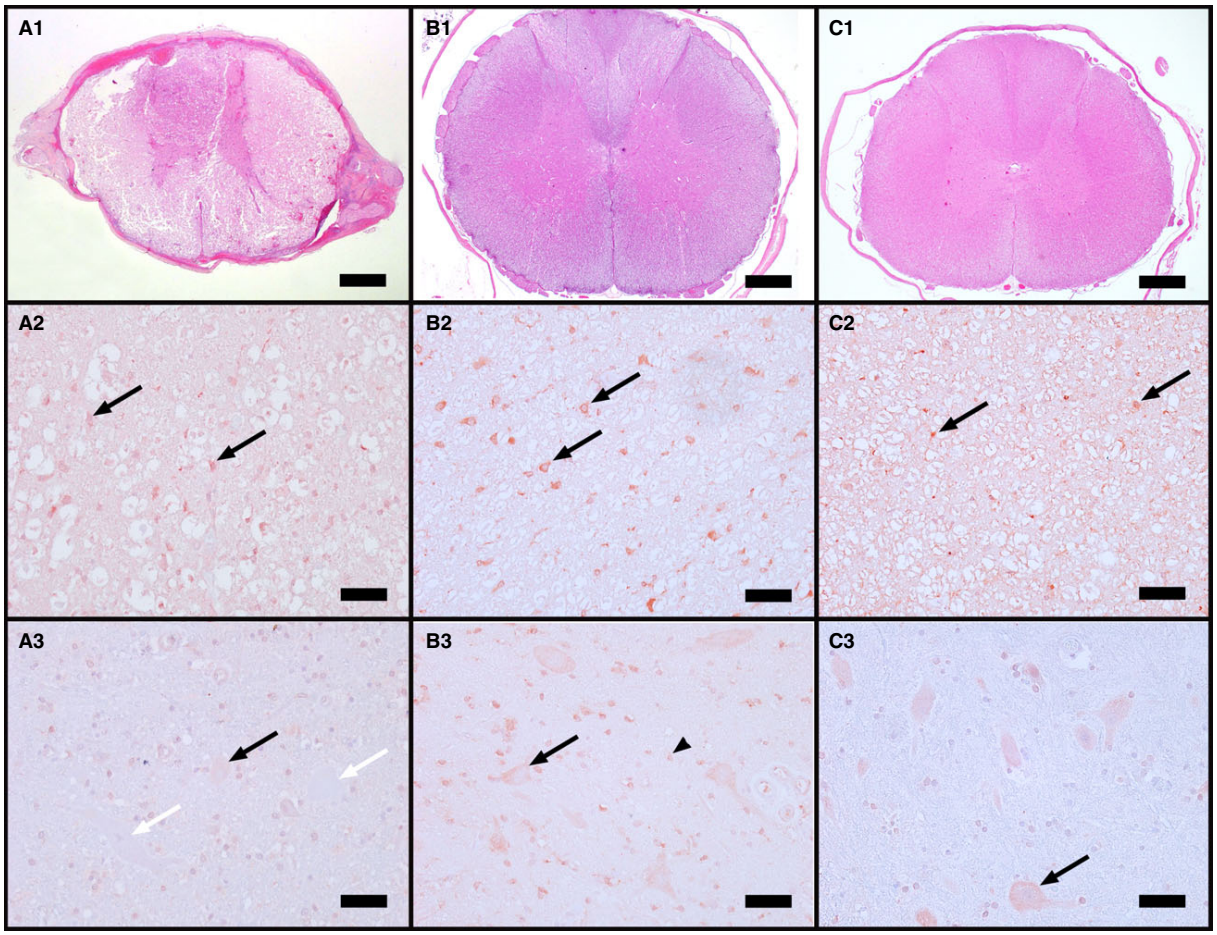

Fig 2. Transverse canine spinal cord sections at the level of the center (**A**) and in a remote segment of an affected (**B**), and of a control dog (**C**), and respective H/E staining of the same areas (**A1–C1**) (H&E, bar = 1000 μm). Immunohistochemistry for endothelin-1 (ET-1) in white matter astrocytes (black arrows) reveals increasing ET-1 expression from control dogs (**C2**) over affected dogs in the center (**A2**) to affected dogs in remote segments (**B2**). Neurons in the center (**A3**) displayed often no (white arrows) or only mild positive staining (black arrow) compared to control dogs with the majority of cells being positively labeled (black arrow). Also astrocytes in the gray matter were positively stained for ET-1 (**B3**, black arrowhead). (A2,3–C2,3: IHC, bar = 50 μm)

myelomalacia in 11 dogs, and extended over more than 3 segments of the spinal cord (ADMM) in 14 dogs (Table 1).

Intramedullary hemorrhage was frequently observed with the largest extent in the center and often more pronounced in the gray than in the white matter. Hemorrhage was already found in acute cases where it obviously started as perivascular leakage of erythrocytes leading to ring hemorrhages. In more advanced cases, the endothelial layer exhibited signs of degeneration. In chronic cases, revascularization became a prominent feature, whereas hemorrhage resolved. Four dogs

showed no hemorrhage, 10 dogs revealed scattered ring hemorrhages (grade 1), 13 dogs diffuse spread of erythrocytes into the parenchyma (grade 2), and 7 dogs displayed mass hemorrhages (grade 3) in the center (Table 1).

The remote segments were histopathologically normal in 18/34 dogs (Fig 2B1), revealed mild white matter damage (scattered spheroids or axonal loss) in 10/34 dogs, mild damage in or around the central canal in 5/34 dogs, and in 1 dog all of the gray matter displayed hemorrhagic necrosis. Besides the latter dog, the majority of cases revealed no intramedullary hemorrhage in the remote segments. Only 3 dogs showed scattered ring hemorrhages, and 3 dogs had some hemorrhagic debris within the central canal.

Assessment of Immunohistochemistry

Endothelin-1 immunoreactivity was observed in both affected and control dogs (Fig 2). Staining varied in respect to intensity and number of positive cells per selected microscopic field. In general, astrocytes of the white matter revealed the most consistent and strongest intensity of staining, followed by neurons. In astrocytes, staining was diffusely cytoplasmatic also involving cell processes (Fig 3B, Fig 2A2–C2). In neurons, staining was distinct granular in the cytoplasm (Fig 1D, Fig 2A3–C3). Endothelial cells were only rarely mildly or moderately positive (Fig 3C). Additionally, in areas of malacia, which generally contained vast numbers of gitter cells, many macrophages were strongly labeled with a granular cytoplasmatic pattern and on cell membranes (Fig 3D). Ependymal cells were occasionally positively labeled, and neutrophils were not stained.

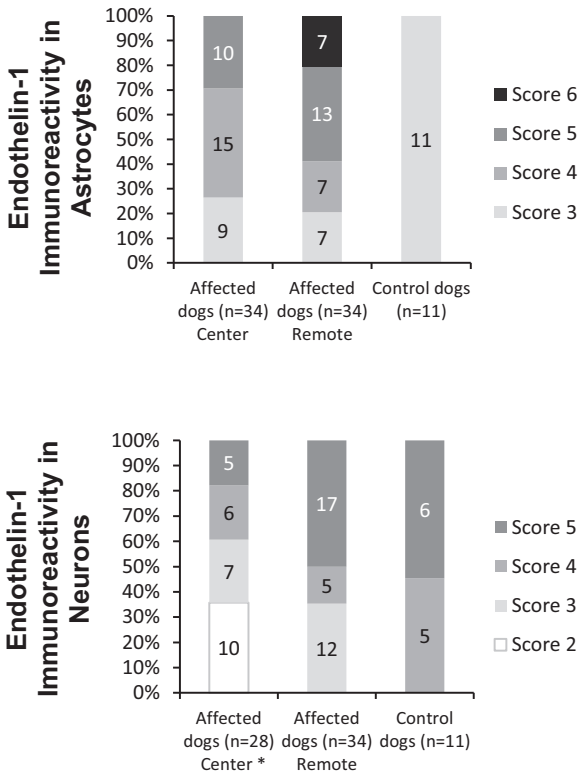

Fig 4. The endothelin-1 immunoreactivity in astrocytes and neurons was expressed as scores and calculated by summation of the grades of number and intensity (eg, ET-1 immunoreactivity in astrocytes = grade "number of positively stained astrocytes" + grade "intensity of astrocytic staining"). These scores were used for further statistics. * Only 28 cases with present neurons on cross section are included.

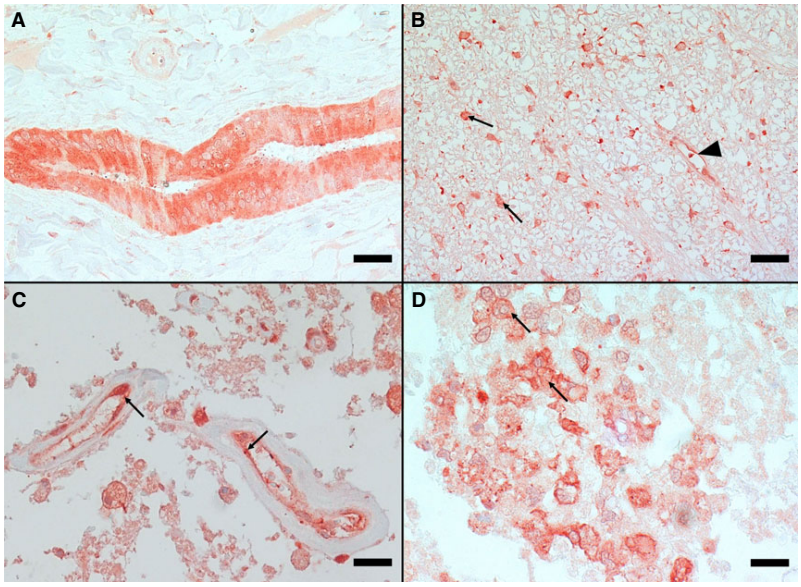

Fig 3. Immunohistochemistry for endothelin-1 of canine liver (**A**) and spinal cord (**B–D**) tissue. **A**—Marked immunostaining of bile duct in liver serving as positive control (IHC, bar = 50 μm); **B**—Spinal cord white matter with strongly stained astrocytes (arrows) and a small capillary with positively stained endothelial cells (arrowhead) (IHC, bar = 50 μm); **C**—Severely necrotic area in the center of the lesion with small vessels with positively stained endothelial cells (arrows) (IHC, bar = 20 μm); and **D**—Positively stained macrophages (arrows) (IHC, bar = 20 μm).

In the center of 14/34 dogs, the spinal cord was completely necrotic. Therefore, the closest adjacent section with adequately preserved tissue (at least 3 visual fields in the white matter without malacia) was used (Fig 2A1-3). The results of the semiquantitative IHC analysis regarding number/percentage of positively stained astrocytes/neurons and the intensity of staining is presented in Figure 9 and in Table S1. The final ET-1 immunoreactivity score (after summation of number and intensity grades) of astrocytes and neurons is shown in Figure 4 and in Table S1.

In negative control slides, staining of neurons, astrocytes, macrophages, and endothelial cells was negative.

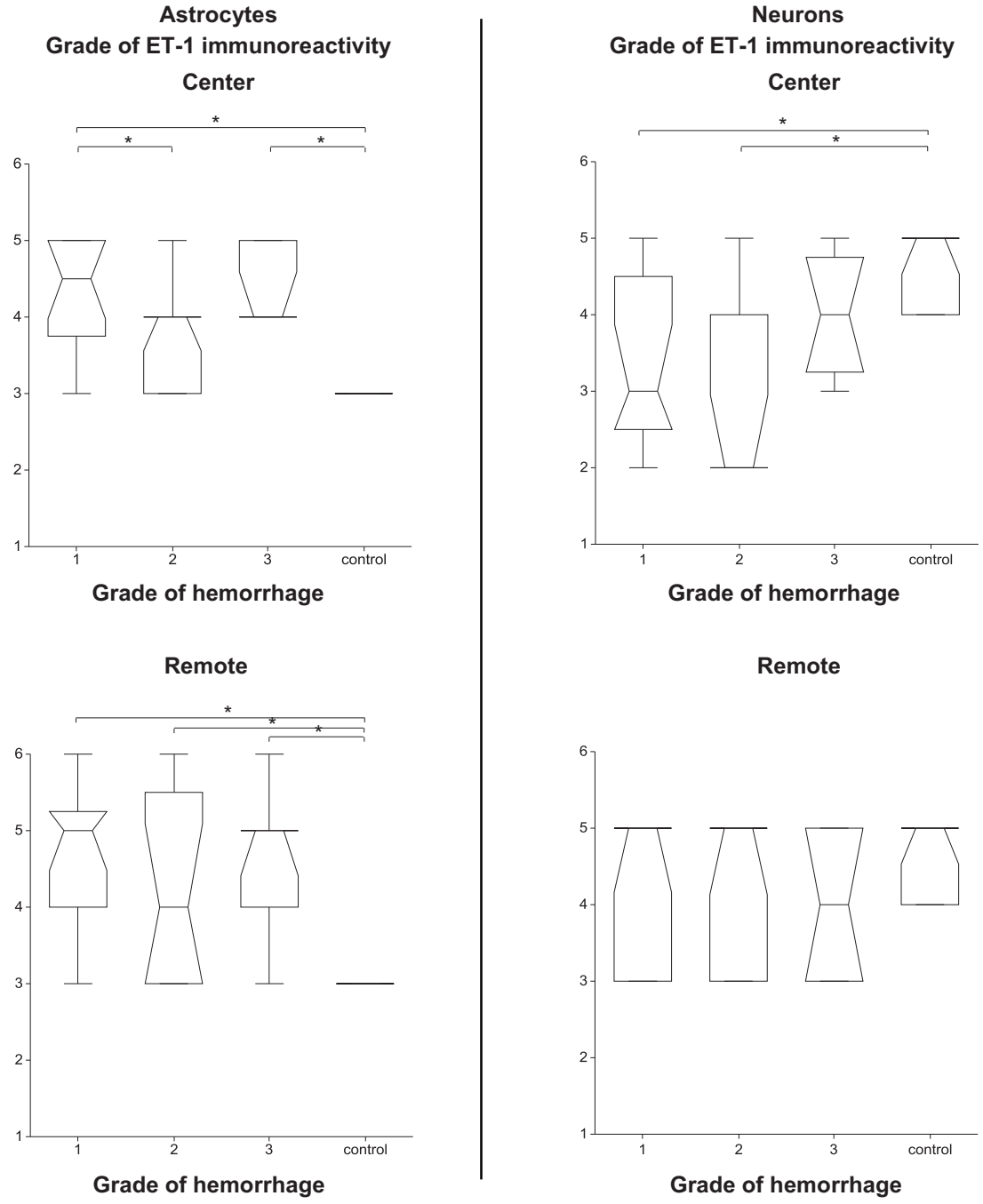

Fig 5. Associations between the endothelin-1 immunoreactivity of astrocytes and neurons at the center and in segments remote from the center and the degree of hemorrhage. The box represents the 25th, 50th, and 75th percentile of the distribution; the whiskers approximate the 5th–95th percentile range. (* indicates values of $P < .05$).

Statistical Analyses

Association between ET-1 Immunoreactivity and Grade of Intramedullary Hemorrhage. In astrocytes, ET-1 immunoreactivity was significantly higher in dogs with hemorrhage than in control dogs both at the level of IVD extrusion and in segments remote from the IVD extrusion (both $P < .001$) (Fig 5).

In neurons, ET-1 immunoreactivity was significantly lower at the level of IVD extrusion in dogs with no/minimal and moderate hemorrhage than in control dogs

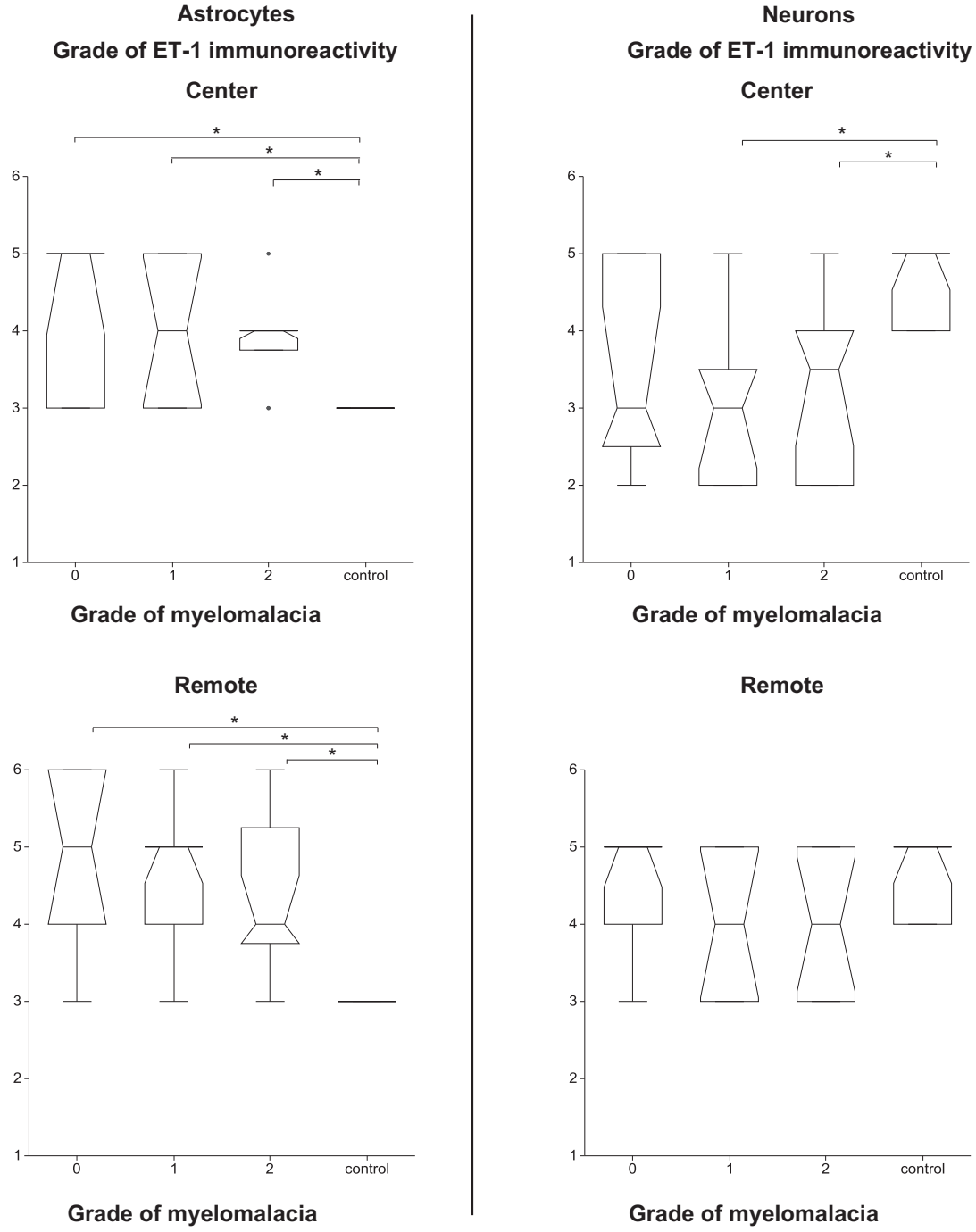

Fig 6. Associations between the endothelin-1 immunoreactivity of astrocytes and neurons at the center and in segments remote from the center and the degree of myelomalacia. The box represents the 25th, 50th, and 75th percentile of the distribution; the whiskers approximate the 5th–95th percentile range. (* indicates values of $P < .05$)

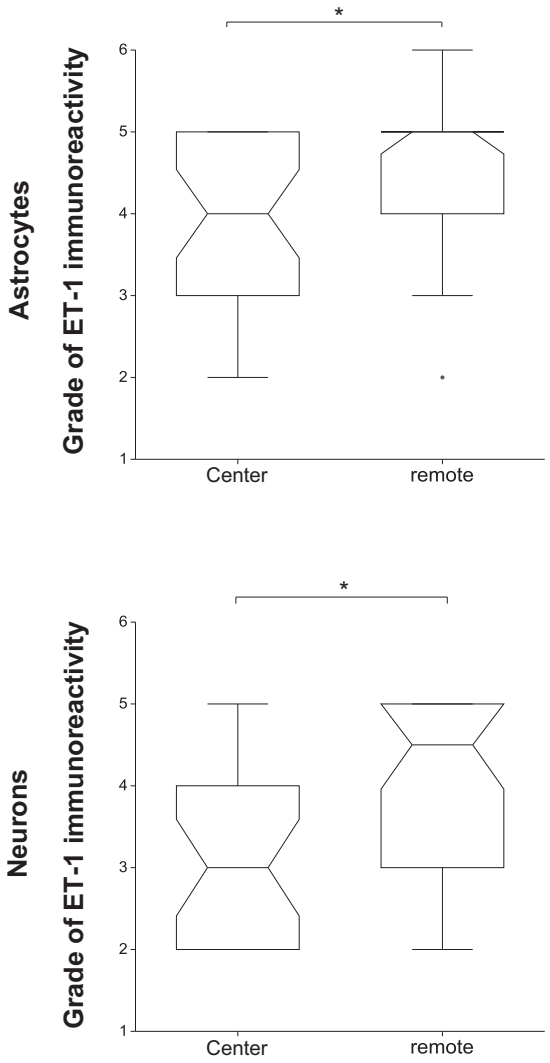

Fig 7. Comparison between the endothelin-1 immunoreactivity in the center to the immunoreactivity in segments remote from the center. The endothelin-1 immunoreactivity of astrocytes and neurons is significantly higher remote from the center ($P = .013$, $P = .001$, respectively). The box represents the 25th, 50th, and 75th percentile of the distribution; the whiskers approximate the 5th–95th percentile range.

($P = .004$), but not different to the control dogs in segments remote from the IVD extrusion ($P = .355$) (Fig 5).

Association between ET-1 Immunoreactivity and Extension of Myelomalacia. In astrocytes, ET-1 immunoreactivity was significantly higher in affected dogs both at the level of IVD extrusion and in segments remote from the IVD extrusion than in control dogs irrespective of the grade of myelomalacia ($P = .001$, $P < .001$, respectively) (Fig 6).

In neurons, ET-1 immunoreactivity was significantly lower in dogs with focal myelomalacia and ADMM than in control dogs at the level of IVD extrusion ($P = .008$), but not different to the control dogs in segments remote from the IVD extrusion ($P = .161$) (Fig 6).

Longitudinal Distribution of ET-1 in Spinal Cord. In both astrocytes and neurons, ET-1 immunoreactivity was significantly lower at the level of IVD extrusion than in segments remote from the IVD extrusion ($P = .013$, $P = .001$, respectively) (Fig 7).

In controls, ET-1 immunoreactivity was equally distributed longitudinally.

Association between ET-1 immunoreactivity and duration of clinical signs. No association was found between ET-1 immunoreactivity and duration of clinical signs.

***Descriptive evaluation of in situ* hybridization.** Endothelin-1 mRNA was present in nearly all neurons in the region of the center as well as remote from the center (Fig 8B–D). However, the intensity of staining was very variable (also between sections of one case on the same slide). Additionally, a few endothelial cells were mildly stained (Fig 8B). Astrocytes, macrophages and neutrophils were not stained in ISH.

Also in control dogs, only neurons displayed ET-1 mRNA.

Staining of canine liver tissue with the labeled sense probe was negative (negative control) and with the labeled antisense probe positive (positive control) (Fig 8A).

Discussion

In IVD extrusion in dogs, intramedullary hemorrhage is a frequent finding, and is associated with longitudinal extension of myelomalacia.[5] The precise pathomechanisms of such ADMM remain uncertain. In view of the proposed involvement of increased ET-1 expression in experimental SCI in small rodents[17,18] and the known stimulating effect of blood products, in particular oxyhemoglobin, on ET-1 production,[25] we evaluated both mRNA and peptide immunoreactivity of ET-1 in intact and injured canine spinal cord after IVD extrusion using ISH and IHC.

The aim of this study was to investigate whether ET-1 immunoreactivity is enhanced in the spinal cord after IVD extrusion, and if so, whether this could be positively associated with intramedullary hemorrhage and tissue destruction.

Endothelin-1 was expressed by astrocytes, macrophages and neurons and only rarely by endothelial cells in all dogs. In astrocytes at the center, ET-1 immunoreactivity was significantly higher in affected dogs than in control dogs irrespective of the grade of hemorrhage or myelomalacia. ET-1 immunoreactivity in neurons at the center was lower than in control dogs. In both astrocytes and neurons, there was a higher ET-1 immunoreactivity in spinal cord regions remote from the center than in the center itself. ET-1 mRNA was present in nearly all neurons with variable intensity, but not in astrocytes. As described in the normal human spinal cord,[34] we could detect mRNA as well as peptide expression of ET-1 in various cell types both in intact and injured spinal cord of dogs. However, in line with the literature, ISH was usually not congruent with IHC. In contrast to the strong mRNA immunoreactivity in nearly all neurons (Fig 8B–D), ET-1 IHC was positive

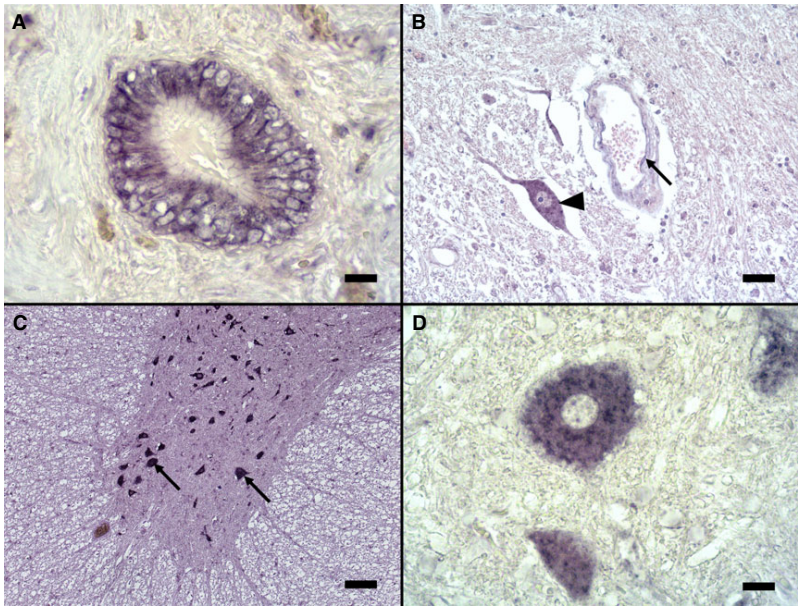

Fig 8. In situ hybridization for endothelin-1 of canine liver (**A**) and spinal cord (**B**–**D**) tissue. **A**—Bile duct of the liver serving as positive control (ISH, bar = 20 μm); **B**—Spinal cord gray matter with strongly stained neuron (arrowhead) and a small capillary with mildly positively stained endothelial cells (arrow) (ISH, bar = 50 μm); **C**—Ventral horn of the spinal cord of an affected dog with multiple neurons. Astrocytes in the adjacent white matter (asterisk) were not stained (ISH, bar = 100 μm); **D**—Positively stained neuron in larger magnification (ISH, bar = 20 μm).

in only one-third of the affected animals at the site of IVD extrusion and in 75% of control animals (Fig 2A3–C3, Fig 9). Also in humans, only 20% of neurons in normal spinal cord were weakly stained for the peptide.[34]

In reverse, astrocytes were consistently immunostained for ET-1 (Fig 2A2–C2), but we could not detect mRNA in these cells in our dogs including 11 chronic cases with active gliosis (Fig 8C). This is at variance with the findings in a murine model where ET-1 mRNA was detected in astrocytes in the process of active gliosis,[24,35] and binding of the peptide ET-1 to ET_B receptor in astrocytes lead to their activation.[35] On the other hand, in rats, it has been shown that there is no simultaneous ET-1 mRNA elevation when the ET-1 peptide in astrocytes is increased,[36] and that increased ET-1 immunoreactivity in astrocytes and endothelial cells occurs even though the mRNA level before and after SCI remained constant.[27,37] It is postulated that ET-1 production in rat astrocytes is mainly post-transcriptionally regulated in response to thrombin stimulation.[36] In view of the inherent instability of mRNA it is clear that the vagaries of ISH are also caused by technical factors such as autolysis, fixation, embedding and storage. Therefore, we refrained from evaluating ISH staining intensity and focused only on its cellular and anatomical localization. Reliable quantitative assessment would require fresh material taken at predetermined intervals, which would be difficult in clinical cases.

We also found marked ET-1 immunoreactivity in macrophages which is consistent with the finding that human macrophages synthesize and secrete ET-1,[38,39] but in contrast to human neutrophils which are able to express mRNA of ET-1 and release the mature peptide[40] we could not detect ET-1 in canine neutrophils.

Comparing injured to normal spinal cord of control dogs, we detected a significantly lower ET-1 immunoreactivity in neurons in the center (Fig 4). Since the gray matter is the initial site of spinal cord damage after mechanical impact and compression, we assume that the decreased ET-1 immunoreactivity in neurons follows the primary injury of these cells which are highly sensitive to ischemia.

In contrast, we found a significantly higher expression of ET-1 in astrocytes of the white matter in the region of the IVD extrusion (Fig 2A2) than in normal spinal cord of control dogs (Fig 2C2). This is consistent with the observations in experimental SCI in small rodents.[37] Additionally, a significant upregulation in both the immunoexpression and number of astrocytes expressing ET_B receptors occurs after experimental SCI in rats, whereas the vascular expression of the ET_A and ET_B receptors remained unchanged,[16] because blocking of ET_B receptors inhibited astrocytic growth after SCI in rats,[37] we conclude that ET-1 has probably an effect on astrocytic proliferation in canine SCI. While it is still unclear if reactive astrogliosis is beneficial or detrimental to neuronal survival and regeneration after SCI, there is evidence to suggest that ET's action on reactive glial cells might promote neurotoxicity.[16,22,41]

Since dogs with IVD extrusion revealed different grades of intramedullary hemorrhage in the center, we

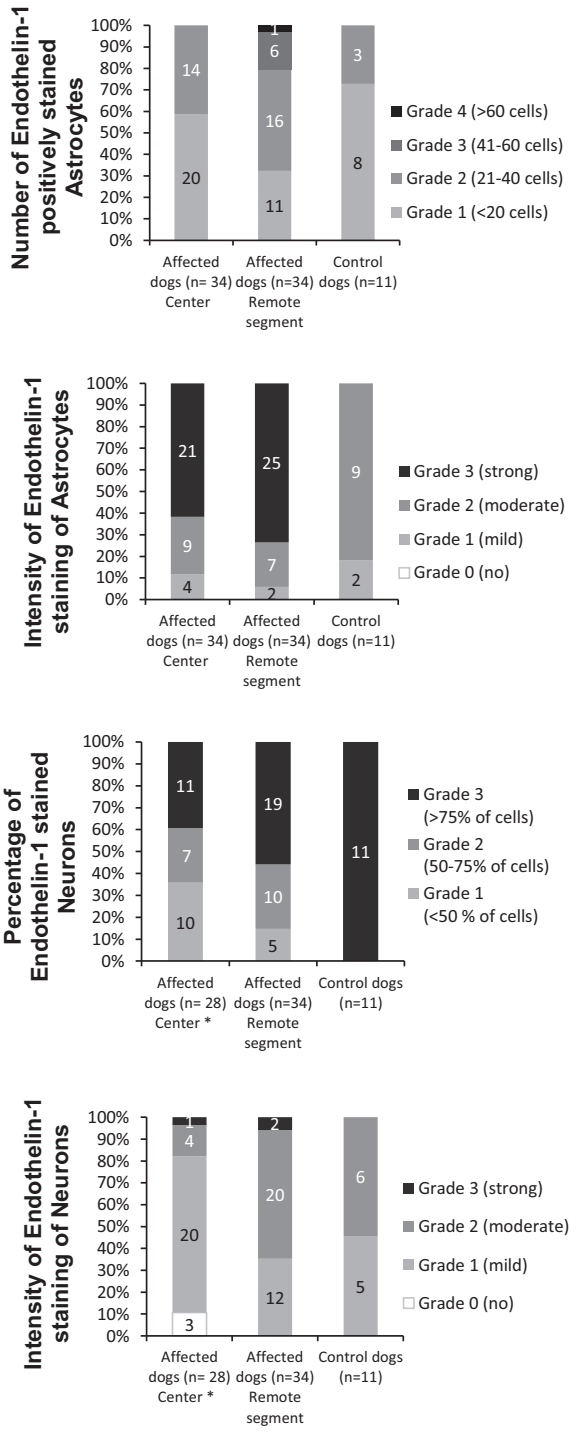

Fig 9. Upper Part—Number of endothelin-1 positively stained astrocytes in 3 randomized visual fields and the intensity of staining expressed in grades 1–4, respectively, and the resulting distribution of grades in the center and remote segments of the spinal cord in affected and in control dogs. Lower Part—Percentage of endothelin-1 positively stained neurons per transverse section of the spinal cord expressed in grades 1–3, the intensity of staining expressed in grades 1–4, and the resulting distribution of grades in the center and remote segments in affected and in control dogs. * Only 28 cases with present neurons on cross-section are included.

could assume in analogy to in vitro models that the initial ET-1 upregulation resulted from the presence of oxyhemoglobin in the lesion.[25] Indeed, we found a positive association between occurrence of hemorrhage and immunoreactivity of ET-1 in astrocytes. However, upregulation of ET-1 in canine IVD disease occurred early after the initial insult and appeared to be sustained over several weeks since we could not detect significant differences between the 3 (acute, subacute, chronic) groups, therefore, besides hemorrhage in the acute stage of the disease other mechanisms are probably involved in continuing expression of ET-1 in SCI.

There was marked upregulation of ET-1 immunoreactivity in astrocytes in spinal cord segments distant from the center (Fig 2B2) which to our knowledge has not been reported in the rodent models of SCI. One possible explanation for this phenomenon could be that ET-1 can act in an autocrine and paracrine way[24,42], thereby activating ET-1 expression in neighboring astrocytes in this way spreading expression to distant areas. Also, in view of the already mentioned fact that blood products are powerful inducers of ET-1, another possible route of spreading ET-1 is hemorrhagic cord debris including macrophages frequently extending rostrally and caudally from the initial injury site through the central canal and subdural space.[5]

Even though we found an association between longitudinal extension of myelomalacia and ET-1 immunoreactivity (Fig 6), a causal association between ET-1 upregulation in astrocytes and progression of cord damage remains to be proven. While the literature on SCI generally emphasizes the detrimental effects of ET-1 excess, this compound could also have beneficial effects. For example, ET-1 stimulates the formation of heme oxygenase-1 whose products (bile pigments) have antioxidative effects to protect the central nervous system against free radicals.[8] Endothelin-1 exerts direct angiogenic activities on endothelial cells by promoting proliferation and migration of endothelial cells. In addition, ET-1 has indirect angiogenic activities by inducing vascular endothelial growth factor production by endothelial cells and vascular smooth muscle cells.[38,42–44]

Assuming that negative effects prevail, ET-1 upregulation could be directly involved in the progression of myelomalacia because of its potent vasoconstrictive effects after binding to ET_{B1} receptors in smooth muscle cells of arterioles resulting in ischemia-induced cell death,[19] or because ET-1 induces release of neurotoxic molecules like glutamate resulting in neuronal cell death.[45,46] Additionally, damage might be inflicted because of the involvement of ET-1 in BSCB breakdown,[12,17] activation of nociceptive neurons,[47] and induction of several inflammatory mediators in neutrophils and macrophages.[38,40]

Our observation of enhanced ET-1 immunoreactivity spreading over multiple spinal cord segments could help to explain the pathogenesis of ADMM. However, we did not detect a linear correlation between ET-1 immunoreactivity and severity of spinal cord damage. While this point requires further studies with more effective quantitative techniques and larger case

numbers, it is very likely that additional multiple factors are involved in longitudinal spreading of myelomalacia after IVD extrusion. Nevertheless, it might be worthwhile to further explore therapeutic options targeting ET-1 expression like ET receptor antagonists and endothelin converting-enzyme inhibitors to reduce the ET-1-induced ischemia and astrogliosis, and to increase neuronal survival, regeneration and function.[48–50]

Acknowledgments

Conflict of Interest Declaration. Authors declare no conflict of interest.

Off-label Antimicrobial Declaration. Authors declare no off-label use of antimicrobials.

References

1. Jeffery ND, Levine JM, Olby NJ, et al. Intervertebral disk degeneration in dogs: Consequences, diagnosis, treatment, and future directions. J Vet Intern Med 2013;27:1318–1333.

2. Henke D, Vandevelde M, Doherr MG, et al. Correlations between severity of clinical signs and histopathological changes in 60 dogs with spinal cord injury associated with acute thoracolumbar intervertebral disc disease. Vet J 2013;198:70–75.

3. Griffith IR. The extensive myelopathy of intervertebral disc protrusions in dogs ("the ascending syndrome"). J Small Animal Pract 1972;13:425–437.

4. Olby N, Levine J, Harris T, et al. Long-term functional outcome of dogs with severe injuries of the thoracolumbar spinal cord: 87 cases (1996–2001). J Am Vet Med Assoc 2003;222:762–769.

5. Henke D, Gorgas D, Doherr MG, et al. Longitudinal extension of myelomalacia by intramedullary and subdural hemorrhage in a canine model of spinal cord injury. Spine J. 2016 Jan 1;16: 82–90. [Epub print ahead].

6. Dumont RJ, Okonkwo DO, Verma S, et al. Acute spinal cord injury, part I: Pathophysiologic mechanisms. Clin Neuropharmacol 2001;24:254–264.

7. Olby N. The pathogenesis and treatment of acute spinal cord injuries in dogs. Vet Clin North Am Small Anim Pract 2010;40:791–807.

8. Sinescu C, Popa F, Grigorean VT, et al. Molecular basis of vascular events following spinal cord injury. J Med Life 2010;3:254–261.

9. Gerzanich V, Woo SK, Vennekens R, et al. *De novo* expression of Trpm4 initiates secondary hemorrhage in spinal cord injury. Nat Med 2009;15:185–191.

10. Simard JM, Woo SK, Aarabi B, et al. The Sur1-Trpm4 channel in spinal cord injury. J Spine. 2013 Aug 17;Suppl 4:002.

11. Kurland DB, Tosun C, Pampori A, et al. Glibenclamide for the treatment of acute CNS injury. Pharmaceuticals 2013;6:1287–1303.

12. Mautes AE, Weinzierl MR, Donovan F, et al. Vascular events after spinal cord injury: Contribution to secondary pathogenesis. Phys Ther 2000;80:673–687.

13. Kuddus RH, Nalesnik MA, Subbotin VM, et al. Enhanced synthesis and reduced metabolism of endothelin-1 (ET-1) by hepatocytes–an important mechanism of increased endogenous levels of ET-1 in liver cirrhosis. J Hepatol 2000;33:725–732.

14. Li J, Guan J, Long X, et al. Endothelin-1 Upregulates the Expression of High Mobility Group Box 1 in Human Bronchial Epithelial Cells. Pharmacology 2015;96:144–150.

15. Tobe S, Kohan DE, Singarayer R. Endothelin receptor antagonists: New hope for renal protection? Curr Hypertens Rep 2015;17:57.

16. Peters CM, Rogers SD, Pomonis JD, et al. Endothelin receptor expression in the normal and injured spinal cord: Potential involvement in injury-induced ischemia and gliosis. Exp Neurol 2003;180:1–13.

17. Westmark R, Noble LJ, Fukuda K, et al. Intrathecal administration of endothelin-1 in the rat: Impact on spinal cord blood flow and the blood-spinal cord barrier. Neurosci Lett 1995;192:173–176.

18. Unic A, Derek L, Hodak N, et al. Endothelins – clinical perspectives. Biochemia Medica 2011;21:231–242.

19. Macrae IM, Robinson MJ, Graham DI, et al. Endothelin-1-induced reductions in cerebral blood flow: Dose dependency, time course, and neuropathological consequences. J Cereb Blood Flow Metab 1993;13:276–284.

20. Zimmermann M, Seifert V. Endothelin and subarachnoid hemorrhage: An overview. Neurosurgery 1998;43:863–875; discussion 875-866.

21. Supattapone S, Simpson AW, Ashley CC. Free calcium rise and mitogenesis in glial cells caused by endothelin. Biochem Biophys Res Commun 1989;165:1115–1122.

22. Sasaki Y, Takimoto M, Oda K, et al. Endothelin evokes efflux of glutamate in cultures of rat astrocytes. J Neurochem 1997;68:2194–2200.

23. Koyama Y, Mizobata T, Yamamoto N, et al. Endothelins stimulate expression of cyclooxygenase 2 in rat cultured astrocytes. J Neurochem 1999;73:1004–1011.

24. MacCumber MW, Ross CA, Snyder SH. Endothelin in brain: Receptors, mitogenesis, and biosynthesis in glial cells. Proc Natl Acad Sci USA 1990;87:2359–2363.

25. Cocks TM, Malta E, King SJ, et al. Oxyhaemoglobin increases the production of endothelin-1 by endothelial cells in culture. Eur J Pharmacol 1991;196:177–182.

26. McKenzie AL, Hall JJ, Aihara N, et al. Immunolocalization of endothelin in the traumatized spinal cord: Relationship to blood-spinal cord barrier breakdown. J Neurotrauma 1995;12:257–268.

27. Siren AL, Knerlich F, Schilling L, et al. Differential glial and vascular expression of endothelins and their receptors in rat brain after neurotrauma. Neurochem Res 2000;25:957–969.

28. Jiang MH, Hoog A, Ma KC, et al. Endothelin-1-like immunoreactivity is expressed in human reactive astrocytes. NeuroReport 1993;4:935–937.

29. Jeffery ND, Smith PM, Lakatos A, et al. Clinical canine spinal cord injury provides an opportunity to examine the issues in translating laboratory techniques into practical therapy. Spinal Cord 2006;44:584–593.

30. Sharma HS. Early microvascular reactions and blood-spinal cord barrier disruption are instrumental in pathophysiology of spinal cord injury and repair: Novel therapeutic strategies including nanowired drug delivery to enhance neuroprotection. J Neural Transm 2011;118:155–176.

31. Karli P, Martle V, Bossens K, et al. Dominance of chemokine ligand 2 and matrix metalloproteinase-2 and -9 and suppression of pro-inflammatory cytokines in the epidural compartment after intervertebral disc extrusion in a canine model. Spine J 2014;14:2976–2984.

32. Young ID, Stewart RJ, Ailles L, et al. Synthesis of digoxigenin-labeled cRNA probes for nonisotopic *in situ* hybridization using reverse transcription polymerase chain reaction. Biotech Histochem 1993;68:153–158.

33. Chen P, Shibata M, Zidovetzki R, et al. Endothelin-1 and monocyte chemoattractant protein-1 modulation in ischemia and human brain-derived endothelial cell cultures. J Neuroimmunol 2001;116:62–73.

34. Giaid A, Gibson SJ, Ibrahim BN, et al. Endothelin 1, an endothelium-derived peptide, is expressed in neurons of the human

spinal cord and dorsal root ganglia. Proc Natl Acad Sci USA 1989;86:7634–7638.

35. Davenport AP. International Union of Pharmacology. XXIX. Update on endothelin receptor nomenclature. Pharmacol Rev 2002;54:219–226.

36. Ehrenreich H, Costa T, Clouse KA, et al. Thrombin is a regulator of astrocytic endothelin-1. Brain Res 1993;600:201–207.

37. Uesugi M, Kasuya Y, Hama H, et al. Endogenous endothelin-1 initiates astrocytic growth after spinal cord injury. Brain Res 1996;728:255–259.

38. Ehrenreich H, Anderson RW, Fox CH, et al. Endothelins, peptides with potent vasoactive properties, are produced by human macrophages. J Exp Med 1990;172:1741–1748.

39. Massai L, Carbotti P, Cambiaggi C, et al. Prepro-endothelin-1 mRNA and its mature peptide in human appendix. Am J Physiol Gastrointest Liver Physiol 2003;284:G340–G348.

40. Cambiaggi C, Mencarelli M, Muscettola M, et al. Gene expression of endothelin-1 (ET-1) and release of mature peptide by activated human neutrophils. Cytokine 2001;14:230–233.

41. Uesugi M, Kasuya Y, Hayashi K, et al. SB209670, a potent endothelin receptor antagonist, prevents or delays axonal degeneration after spinal cord injury. Brain Res 1998;786:235–239.

42. Mencarelli M, Pecorelli A, Carbotti P, et al. Endothelin receptor A expression in human inflammatory cells. Regul Pept 2009;158:1–5.

43. Bagnato A, Spinella F. Emerging role of endothelin-1 in tumor angiogenesis. Trends Endocrinol Metab 2003;14:44–50.

44. Tykocki NR, Watts SW. The interdependence of endothelin-1 and calcium: A review. Clin Sci 2010;119:361–372.

45. Kobayashi T, Oku H, Fukuhara M, et al. Endothelin-1 enhances glutamate-induced retinal cell death, possibly through ETA receptors. Invest Ophthalmol Vis Sci 2005;46:4684–4690.

46. Zampronio AR, Kuzmiski JB, Florence CM, et al. Opposing actions of endothelin-1 on glutamatergic transmission onto vasopressin and oxytocin neurons in the supraoptic nucleus. J Neurosci 2010;30:16855–16863.

47. Smith TP, Smith SN, Sweitzer SM. Endothelin-1 induced desensitization in primary afferent neurons. Neurosci Lett 2014;582:59–64.

48. McLarnon JG, Wang X, Bae JH, et al. Endothelin-induced changes in intracellular calcium in human microglia. Neurosci Lett 1999;263:9–12.

49. Chou AK, Chen TI, Winardi W, et al. Functional neuroprotective effect of CGS 26303, a dual ECE inhibitor, on ischemic-reperfusion spinal cord injury in rats. Exp Biol Med 2007;232:214–218.

50. Gong S, Peng L, Yan B, et al. Bosentan reduces neuronal apoptosis following spinal cord ischemic reperfusion injury. Spinal Cord 2014;52:181–185.

Supporting Information

Additional Supporting Information may be found online in the supporting information tab for this article:

Table S1. Part 1—Number of endothelin-1 positively stained astrocytes in 3 randomized visual fields and the intensity of staining expressed in grades 1–4, respectively, and the resulting distribution of grades in the center and remote segments of the spinal cord in affected and in control dogs; Part 2—Percentage of endothelin-1 positively stained neurons per transverse section of the spinal cord expressed in grades 1–3, the intensity of staining expressed in grades 1–4, and the resulting distribution of grades in the center and remote segments in affected and in control dogs; Part 3—The endothelin-1 immunoreactivity (final score) in astrocytes and neurons was calculated by summation of the grades of number/percentage and intensity (eg, ET-1 immunoreactivity score in astrocytes = grade "number of positively stained astrocytes" + grade "intensity of astrocytic staining"). These scores were used for further statistics. * Only 28 cases with present neurons on cross-section are included.